

Dust Distribution in Gas Disks II: Self Induced Ring Formation Through a Clumping Instability

Hubert Klahr¹ and D.N.C. Lin

UCO/Lick Observatory, University of California, Santa Cruz, CA 95064

VERSION: Friday, Feb. 25th 2005

STATUS : ApJ resubmitted after first referee report

ABSTRACT

Debris rings of dust are found around young luminous stars such as HR4796A and HD141569. Some of these entities have sharp edges and gaps which have been interpreted as evidence for the presence of shepherding and embedded planets. Here we show that gaps and sharp edges in the debris disks of dust can also be spontaneously self generated if they are embedded in optically thin regions of gaseous disks. This clumping instability arises in regions where an enhancement in the dust density leads to local gas temperature and pressure increases. Consequently, the relative motion between the gas and the dust is modified. The subsequent hydrodynamic drag on the dust particles leads to further enhancement of their concentration. We show that this process is linearly unstable and leads to the formation of ring-like structures within the estimated life time of such young objects. Once the gas is removed (e.g. by photo evaporation) the structures are “frozen” and will persist, even when the gas might not be observable anymore.

Subject headings: circumstellar matter – planetary systems – stars: formation

1. Introduction

The coplanar orbits of nearly all planets in the Solar System inspired Laplace to propose that they are formed in a gaseous disk, the primordial solar nebula, centered around the protosun. Protoplanetary disks are found around a large fraction of classical and weak-line

¹present address: Max-Planck-Institut fuer Astronomie, Heidelberg, Germany

T Tauri stars (Stauffer, Prosser, Hartmann, & McCaughrean 1994). The existence of these disks is generally inferred from the excess in the infrared continuum which is primarily due to dust reprocessing of the stellar radiation. These signatures fade with the age of the stars. In young stellar clusters, the fraction of stars with clear signs of infrared excess declines with their age on the time scale of a few Myr (Haisch, Lada, & Lada 2001). Around some post T Tauri stars such as β Pic, debris disks have been found. The amount of dust which emits infrared radiation in these debris disks also appears to be inversely proportional to the age of their host stars (Zuckerman, Kim, & Liu 1995). This apparent evolutionary pattern may be interpreted as coagulation of dusty material into relatively large particles (McCabe *et al.* 2003) which are less efficient in reprocessing the stellar radiation (Yorke & Sonnhalter 2002). It is also possible that the residual grains are depleted from the circumstellar disks by photo evaporation, stellar wind, or some dynamical processes. In either case, the decrease in the infrared excess casts a constraint on the magnitude of time scale for planet formation to be in the range of a few million years.

Current searches for extra solar planets indicate that they are present in at least eight percent of all target stars (Marcy, Butler, & Vogt 2000). As data accumulate with increasing time bases, the discoveries of long period planets are anticipated around a much larger fraction of all planets (Trilling, Lunine, & Benz 2002, Armitage *et al.* 2002, Ida & Lin 2003). If so, some debris disks may indeed contain newly formed protoplanets since they represent advanced evolutionary stages of protostellar disks. These planets are expected to tidally interact with their ambient gas and dust by exciting density waves (Goldreich & Tremaine 1982, Papaloizou & Lin 1984), inducing gaps with sharp edges (Borderies, Goldreich & Tremaine 1989, Lin & Papaloizou 1986, Artymowicz, & Lubow 1994, Bryden, Ro'zyczka, Lin, & Bodenheimer 2000), confining rings between them (Bryden, Chen, Lin, Nelson, & Papaloizou 1999), and warping the disk (Larwood, & Papaloizou 1997).

The discovery of a debris disk around HR4796A was particularly interesting because its sharp edges resemble that expected for tidally truncated disks (Schneider *et al.* 1999). Recent HST image of another disk around HD141569 clearly indicate that its outer region is strongly perturbed by its binary companion (Clampin, Ford, Illingworth, Krist & Ardila in preparation). But, this disk appears to be composed of two concentric rings which are separated by a narrow gap (Weinberger *et al.* 1999). The binary star's tidal torque occurs on length scales comparable to the disk radius and are unlikely to induce the formation of the fine structure seen in this disk. A more plausible and potential exciting alternative culprit is a Jupiter-mass planet which may be embedded within the gap (Weinberger *et al.* 1999). But, the distance of the hypothetical planets from their host stars in both cases are more than an order of magnitude larger than that of the gaseous giant planets in the solar system. The dynamical time scale in these disk regions exceeds 10^3 yr. Also in these regions,

the disk may attain sufficient mass to become gravitationally unstable and remain optically thin. The formation of giant planets through gravitational instability may be rapid (Boss 1998) if the fragment can contract and collapse before being sheared out (Pickett, Mejia, Durisen, Cassen, Berry, & Link in press; Pickett, Durisen, Cassen, & Mejia 2000; Nelson, Benz, Adams, & Arnett 1998). The necessary condition for a rapid contraction is that the cooling time scale must be comparable to or shorter than the local dynamical time scale (Johnson & Gammie 2003).

Application of the conventional core-accretion theory of planet formation suggests that the formation time scale for Jovian-mass planets at the large distances of the disks is much longer than the age of HR4796A and HD141569 even under the most favorable conditions (Pollack *et al* 1996). But the discovery of short-period planets (Mayor & Queloz 1995) supports the scenario that planets may migrate over extensive distance shortly after their formation (Goldreich & Tremaine 1980, Ward 1986, Lin & Papaloizou 1986, Lin, Bodenheimer, & Richardson 1996). A particularly effective mechanism for rapid and extensive migration is through a runaway interaction between embedded planets and their nascent (Masset & Papaloizou 2003, Artymowicz in preparation) although the termination conditions remain uncertain. Another potential avenue for extensive outward migration for protoplanets formed within a few AU from their host stars is through distant resonant encounter between several massive planets (Lin & Ida 1997). In the context of the Solar system, Thommes, Duncan, & Levison (2002) suggested that Uranus and Neptune may have migrated outwards as a consequence of the gravitational interaction between the outer planets and residual planetesimals. In general, dynamical instability induces the planets to attain large eccentricities. The gap width induced on the nearby disk by a highly eccentric planetary perturber may be much larger (Artymowicz & Lubow 1996) than that observed between the rings around HD 141569. But, the eccentricity of the perturber may also be rapidly damped by the collective response of the residual planetesimal disk (Agnor & Ward 2002).

The above discussions indicate that despite its potentially profound implication on the theory of planet formation, the planet-disk interaction scenario is highly uncertain. Thus, it is useful to explore some alternative explanations for the observed features in the debris disks. In a previous paper (Klahr & Lin 2001), we suggested that the debris disks and rings may be confined with relatively sharp edges through their interaction with both the stellar radiation and residual gas (see also (Takeuchi & Artymowicz 2001)). Due to a negative pressure gradient in the radial direction, the azimuthal velocity of gaseous disks is generally sub Keplerian everywhere. In opaque regions of the disk, the grains' motion is affected only by the central star's gravity and their interaction with the ambient gas. As they attempt to attain Keplerian orbits, the grains experience a head wind and the hydrodynamic drag resulting from this differential motion leads them to undergo orbital decay (Weidenschilling

1977).

But, in the optically-thin regions of the disk where the grains are directly exposed to the stellar radiation, the azimuthal velocity of the grains may also be reduced by the outwardly pointing radiation pressure from the central star. Around relatively luminous stars, such as HR4796A and HD 141569, the grains' azimuthal velocity may be less than that of the gas such that the combined effects of the radiation pressure and hydrodynamic drag can induce the grain to migrate outward. The above effects require the presence of residual gas which is otherwise difficult to detect directly. For example, at large distances from its central star, CO gas may be depleted as volatile molecules are condensed onto the grains (Thi *et al.* 2002). The detection of molecular hydrogen around some of these debris disks have been reported (Thi *et al.* 2001), although observational uncertainties remain (Sheret, Ramsey-Howat, & Dent 2002).

In the context of the debris disk around HR 4796A, we showed that due to these hydrodynamic drag and radiation pressure, a slight inhomogeneity in the gaseous background can lead to the formation of the dusty rings with sharp edges. Thus, the observed features in the ring do not necessarily imply the presence of embedded planets. Furthermore, if these sharp features are indeed an indicator for some residual gas, a less stringent formation time scale would be required for the formation of gaseous planets in the outskirts of planetary systems (for the formation of Neptune, see Bryden *et al.* 1999).

Nevertheless, gas may have been present at the time when the structures in HR4796A and HD 141569 formed. After the ring structures were created by assistance of the gas, the gas may well have been evaporated and depleted to a level below observability and below a value that would still influence the dust. The dust rings would then be the “frozen” final state of the ring formation process.

In this paper, we extend our previous investigation on the dynamical evolution of optically thin debris disks around relatively luminous stars. In our previous work, we assumed an arbitrary surface density distribution for the gas. Our main objective here is to illustrate that the feedback interaction between the gas and dust naturally lead to a clumping instability in which the dust diffuses into an equilibrium configuration that they become self confined. We show that this clumping instability results naturally and the structure of the debris disks can be determined self consistently. In §2, we outline our basic assumptions and formulate the evolution of both dust and gas. A linear stability analysis in §3 is followed by some numerical models in §4 and their observational signature in §5. We summarize our results and discuss their implications in §6. In the appendix we give a simple estimation for realistic β values (i.e. the sensitivity of gas temperature on grain density).

2. Basic assumptions for the model

We consider an optical thin debris disk where the gas dust plasma that is being irradiated by stellar light. The gas attains an equilibrium temperature somewhere between a maximal and a minimal possible temperature. The maximum temperature is given by the blackbody temperature of the dust grains and the minimum temperature by the ground state of the gas molecules and the temperature of the interstellar space.

2.1. Gas Temperature

The equilibrium temperature of the gas T_g in an optical thin regime at low temperatures is given by the balance between radiative cooling via line emission and heating due to various effects including photoelectric heating via the silicate grains, the gas molecules' inelastic collisions with the dust grains as well as line absorption of UV photons (Kamp & van Zadelhoff 2001; Ferland, Korista, Verner, Ferguson, Kingdon & Verner 1998; Woitke, Krüger & Sedelmayr 1996). The maximum temperature which can be attained by the gas is already given by the temperature of the dust grains, which themselves are heated to blackbody temperature by irradiation from the central star. In the current analysis, we are primarily interested in the interaction between the gas and the dust. We neglect effects such as super-heating of small grains due to radiative inefficiencies (Chiang & Goldreich 1997) for this analysis as it is not important to understand the basic instability.

In general, the gas temperature is a complex function of radius R , luminosity of the central object L_* , surface of the dust grains, surface density of the gas Σ_g , surface density of the dust content Σ_d , A_d is the cross section of the dust, and most of all the complete chemical composition of the gas N_n and the ionization state of the molecules X_n , determining the possible line transitions leading to the cooling emission of radiation:

$$T_g = f(R, L_*, A_d, \Sigma_g, \Sigma_d, N_n, X_n, \dots). \quad (1)$$

The detailed determination of the function f will be presented elsewhere.

For the present purpose of examining the stability of dust to gas interaction, the most important parameter is

$$\beta \equiv \frac{\partial \ln T}{\partial \ln \Sigma_d}. \quad (2)$$

In order to illustrate the evolution of small disturbances, we adopt a simple generic analytic prescription in which we assume that

$$T_g = T_0 \left(\frac{\Sigma_d}{\Sigma_0} \right)^\beta, \quad (3)$$

where β , T_0 and Σ_0 are to be determined later by radiation transfer models. In the linear stability analysis, only the instantaneous slope β needs to be specified and the above explicit prescription for $T_g(\Sigma_d)$ is not needed.

The power index β gives the steepness of the temperature dependence on the dust load. In regions where the dust to gas surface density ratio, $\Sigma_d/\Sigma_g > Z_\odot$, where Z_\odot is the solar metalicity, the disk gas is primarily heated by conduction to the gaseous molecules from the dust particles, which themselves are heated by the irradiation of their host stars and via photoelectric heating via the silicate grains. Qualitatively, T_g is expected to be an increasing function of Σ_d because in the optically thin region of the disk, the fraction of stellar radiation absorbed by the dust is proportional to the optical depth of the dust. The rate of conduction between the gas molecules and the dust grains as well as the number of photoelectric electrons is also an increasing function of Σ_d . Thus, we consider primarily the range of parameter space for which $\beta > 0$ (see appendix). However, in the low Σ_d/Σ_g limit, the gas molecules are mostly heated directly by the UV photons of their host stars such that the energy deposition rate to the disk is insensitive to the magnitude of Σ_d (Kamp *et al.* 2003). Also in the opaque regions of the disk, $T_g = T_d$ and is independent of Σ_d so that $\beta = 0$. Therefore, we also consider other values of β . Under unlikely circumstances where $\beta < 0$, the debris disks are stable against this clumping process.

2.2. Radial Drift velocity

In our previous analysis (Klahr & Lin 2001), we derived the radial drift velocities v_r for particles under the combined influence of non-Keplerian gas motion and radiation pressure. (The velocity of the dust is expressed in lower case v 's whereas that of the gas is expressed in capital letters V 's.) For small particles with radius a_d and density ρ_d which are in the Epstein regime the friction time is $\tau_f = a_d \rho_d / (\rho_g c_s)$ in a gas of density ρ_g and a sound speed of c_s the radial velocity is

$$v_r = \tau_f 2\Omega^* dV^* \quad \text{for } St \ll 1, \quad (4)$$

where the Stokes Number $St = \tau_f \Omega^* \ll 1$, Ω^* is the particles' hypothetical orbital frequency subjected only to the stars' gravity and radiation pressure. The difference of the actual orbital velocity of the disk gas and the hypothetical particle velocity $\Omega^* R$, dV^* , can have either positive or negative signs depending on the structure of the gas disk.

Similarly, the radial drift velocity of the larger particles can be expressed as

$$v_r = dV^* \quad \text{for } St = 1, \quad (5)$$

and

$$v_r = \frac{2dV^*}{\Omega^* \tau_f} \quad \text{for} \quad St \gg 1. \quad (6)$$

We utilize these expression for the radial drift velocities in the linear stability analysis below.

3. Stability Analysis

The evolution of an axis-symmetric dust distribution is determined by the continuity equation in cylindrical coordinates:

$$\frac{\partial}{\partial t} \Sigma_d + \frac{1}{r} \frac{\partial}{\partial r} r \Sigma_d v_r = 0. \quad (7)$$

In general one would have to solve a continuity equation for all single dust species as their radial drift velocity depends on the friction time. Such detailed approach will be carried out in future models which will try to fit the observations in detail. For this work we assume a mono dispersive dust distribution which is characterized by one particle size, shape and friction time.

The radial drift velocity for the most mobile particles ($St = 1$) is:

$$v_r = dV^*, \quad (8)$$

and $dV^* = V_\phi - v_\phi^*$ is a function of the particles theoretical azimuthal velocity v_ϕ^* for circular orbit in the absence of gas

$$v_\phi^* = \sqrt{\frac{GM_\star - \frac{L_\star A_d}{4\pi m_d c}}{r}}. \quad (9)$$

Here A_d is the cross section and m_d the mass of the dust grains. The speed of light is denoted by c .

We want to stress that the characteristic radial drift velocity will also be correct within an order of magnitude for particles which are up to 20 times larger or 20 times smaller than the characteristic size.

The azimuthal velocity of the gas is V_ϕ and is determined by the radial pressure gradient in first order approximation to

$$V_\phi = \Omega r + \frac{1}{2\Omega \Sigma_g} \frac{\partial}{\partial r} P \quad (10)$$

where $\Omega = (GM_\star/r^3)^{1/2}$ is the Keplerian frequency. The pressure P is given by an ideal gas equation of state a function of temperature and gas surface density Σ_g thus:

$$V_\phi = \Omega r + \frac{R_{\text{gas}}}{2\mu\Omega} \left(\frac{T_g}{\Sigma_g} \frac{\partial}{\partial r} \Sigma_g + \frac{\partial}{\partial r} T_g \right) \quad (11)$$

where R_{gas} is the gas constant. Note that the second and third terms on the right hand side of eq(11) are due to the surface density and temperature distribution of the gas respectively. In general, Σ_g is not perturbed by the dust concentration. But any clumping in the dust would lead to a local enhancement in Σ_d which in turn heats the gas. Because the temperature distribution is much more sensitive than the Σ_g distribution, we focus our stability analysis on those contributions which are proportional to the temperature gradient.

Combining all the equations into one expression and defining a local mean sound speed to be $\frac{R_{gas}T_0}{\mu} = c_s^2$, we find:

$$\frac{\partial}{\partial t} \Sigma_d = -\frac{1}{r} \frac{\partial}{\partial r} r \Sigma_d \left[\Omega r + \left(\frac{c_s^2}{2\Omega r} \right) \left(\frac{T_g}{T_0} \right) \left(\frac{\partial \ln \Sigma_g}{\partial \ln r} + \beta \frac{\partial \ln \Sigma_d}{\partial \ln r} \right) - \sqrt{\frac{GM_\star - \frac{L_\star A_d}{4\pi m_{dc}}}{r}} \right]. \quad (12)$$

With a prescription for T_g such as that in eq(3), this continuity equation can be solved numerically.

For the linear stability analysis, we simplify the equation to clarify the mechanism by dropping all terms not important for the instability. We neglect the effects of radiation pressure which gives only a systematic offset but no instability. We also assume that the gas is much more smoothly distributed than the dust, *i.e.* $|\partial \ln \Sigma_g / \partial \ln r| \ll |\partial \ln \Sigma_d / \partial r|$ so that:

$$\frac{\partial}{\partial t} \Sigma_d = -\frac{1}{r} \frac{\partial}{\partial r} \left(\left(\frac{T_g}{T_0} \right) \frac{c_s^2 \beta}{2\Omega} \frac{\partial \ln \Sigma_d}{\partial \ln r} \right). \quad (13)$$

Linearized $\Sigma_d = \Sigma_0 + \Sigma'_d$, we find in a local approximation with $\frac{1}{r} \partial_r r \rightarrow \partial x$ at a given radius $r = R$

$$\frac{\partial}{\partial t} \Sigma'_d + \beta \frac{c_s^2}{2\Omega} \frac{\partial^2}{\partial x^2} \Sigma'_d = 0. \quad (14)$$

The local approximation does not limit the physical validity of our analysis. It only simplifies the maths but does not change the underlying physics. We also could have stucked to the polar coordinate system and used e.g. Bessel functions instead of Fourier modes. The answer would be the same but it would be less transparent. On the other hand ($1/r \partial_r r = \partial_x$) requires at least $x/r \ll 1$ and in the case of HR4796A the radial extent of the ring is 20 AU where the radius is 70 AU, so the approximation is fulfilled.

For short-wavelength disturbances, the above equation has a solution $\Sigma'_d \sim e^{-i(\omega t - kx)}$. The growth-rate of these disturbance is:

$$\Gamma = -i\omega = \beta \frac{c_s^2}{2\Omega} k^2. \quad (15)$$

If we replace $c_s = H\Omega$ and defines $n = kR$ then the above equation reduces to

$$\Gamma = -i\omega = \frac{1}{2}\beta \left(n \frac{H}{R} \right)^2 \Omega. \quad (16)$$

These results indicate that a Σ_g variation can lead to local heating of the gas which in term modifies the local pressure gradient and the azimuthal speed of the gas. Through a hydrodynamic drag, the dust particles respond by clumping together to enhance the local Σ_g . This clumping instability is related by, but not the same as the diffusion and thermal instability in gaseous accretion disks (Pringle 1981). In both cases, the growth of a perturbation is due to the efficiency of angular momentum transfer being inversely proportional to the surface density. But the present clumping instability involves a different physical process which requires the feedback between the gas and the dust through the radiative heating of the dust and the local conductive heating of the gas.

It is interesting to notice that the growth rates are close to the orbital frequency for $\frac{H}{R} \approx \frac{1}{n}$. In this limit, the instability will grow on a dynamical time scale. But, the linear leading-terms approximation is inappropriate for disturbance with $n > R/H$. On these scale, the thin disk approximation breaks down and the gas pressure in the direction normal to the plane has a tendency to stabilize the flow. In addition, very small scale variation, if unstable can reverse the gradient of angular momentum in the disk (see eq 11). A negative angular momentum gradient, even localized can lead to interchange instabilities which results in mixing in the radial direction. Since we are primarily interested in identifying the condition for the onset of a clumping instability, we shall present elsewhere the growth limit due to amplitude saturation and nonlinear effects.

Nevertheless, eventually the gas will be removed from the system (e.g. photo evaporation). As a consequence the friction time of the particles will increase and the radial drift velocity decrease (see eq 6). Thus, the right hand side of eq(13) will eventually vanish. This means that the structure is now in first order approximation constant in time. So even the gas is removed from the system the structure in the dust distribution will remain. Consequently we can not argue that there must still be gas at an observable amount in HR4796A and HD141569.

Note that Γ and β have the same sign. It is not forbidden that β may attain a negative value, in which case the perturbation would be damped. However, this case requires the gas temperature to decrease with Σ_d which seems to be physically unlikely. In the opaque regions of the disk where all radiation is intercepted by the dust, the gas temperature becomes independent of Σ_d so that $\beta = 0$. Even in the optically thin region, if the gas cooling by molecular transition is inefficient compared with its heating due to conduction, T_g may approach to that of T_d so that β also vanishes. In these $\beta = 0$ cases, the perturbation

remains neutral and the disk is stable.

4. Numerical Solution

In order to have an illustration of how the instability can evolve into the non linear region, we obtain numerical solutions of the complete continuity equation 12 without substituting the gas temperature T_g and assuming circular orbits:

$$\frac{\partial}{\partial t} \Sigma_d = -\frac{1}{r} \frac{\partial}{\partial r} \left(r^{-5/2} \frac{\Sigma_d}{\Sigma_g} \frac{\partial}{\partial r} \Sigma_g T_g \right). \quad (17)$$

Here we set all physical constants to one and used $\Omega = r^{-3/2}$. Using these dimensionless units sets the unit time scale to one orbital period at the radius r times the inverse square of the pressure scale height.

$$\tau_0 = \left(\frac{H}{r} \right)^{-2} \frac{2\pi}{\Omega} \quad (18)$$

Thus, it will be simple to calculate the physical time scale for a real object like HR4796A afterwards by simply multiplying the dimensionless time by the unit timescale of the physical radius, that is considered.

The gas temperature is calculated from the power-law prescription for T_g as expressed in eq (3), where we additionally limited the dynamical range of one order of magnitude:

$$T_g = T_0 \max \left[3.33, \min \left[0.33, \left(\frac{\Sigma_d}{\Sigma_0} \right)^\beta \right] \right]. \quad (19)$$

As we will discuss in the appendix the gas temperature will probably stay in these limits (see Figure 1).

The analytic estimate in eq (16) indicates that the growth rate is proportional to n^2 , *i.e.* the most unstable perturbations are those with the smallest wave numbers. We have already indicated above that the thin disk approximation for the continuity equation breaks down for $n > R/H$. In reality, the vertical pressure gradient becomes important to stabilize the disturbance. We also argued that the non linear growth of disturbance with $n > R/H$ would lead to the violation of the Rayleigh's criterion for axis-symmetric rotational flows. If such a situation arises, mixing would almost certainly limit the growth of the clumpy structure. In order to avoid the unphysical growth on scales smaller than H , we introduce a prescription by adding a stabilizing contribution to the continuity equation such that

$$\frac{\partial}{\partial t} \Sigma_d = -\frac{1}{r} \frac{\partial}{\partial r} \left(r^{5/2} \frac{\Sigma_d}{\Sigma_g} \frac{\partial}{\partial r} \Sigma_g T_g - H^2 \frac{\partial}{\partial r} \frac{\partial^2}{\partial r^2} \Sigma_d \right). \quad (20)$$

With this prescription, the equation can now be discretized with central differences on a grid with 100 radial points and 2 ghost cells on each side, where Σ_d was set to fixed values $\Sigma_{inner} = 1.0$ and $\Sigma_{outer} = 10^{-10}$.

Another choice of boundary conditions would have been vanishing gradients. But they lead to numerical problems with the scheme we applied, i.e. negative densities can occur close to the boundary. The application of fixed values for the ghost cells helps to avoid this, whereas the overall ring structures are not changed in size and location.

We developed a stable numerical scheme using a fourth order Runge Kutta integrator to advance the distribution in time. The fixed gas density distribution was chosen to be $\Sigma_g \propto r^{-3/2}$. A similar profile was chosen for initial distribution of the dust Σ_d with a randomly fluctuation of 1% amplitude. We also set $T_0 \propto r^{-1/2}$ with $H = 0.1$.

The stabilizing contribution is the only limit for the growth of the shortest modes in this flat approximation where vertical structure is neglected. A more realistic modeling would require to resolve the 3D structure of the gas disk and the turbulent processes within. Nevertheless, this is way beyond the considerations of this paper. On top of this we would only shift the application of free parameters one layer up, without gaining much additional insight.

A pressure change can lead to the modification in the density distribution in both vertical and radial direction. Since hydrostatic equilibrium is maintained in the vertical direction by a balance between pressure and gravity, a change in the pressure can modify the density distribution above the mid plane. But it does not necessarily change the surface density. In the radial direction, equilibrium is maintained by a balance between centrifugal force of the Keplerian rotation and the stellar gravity. Thus, small variations in the pressure do not modify the gas density significantly.

The linearized solution in eq(16) clearly indicates that the sign of β determines the growth and damping of the disturbances. We choose three values of β (-1, 1, 2) to illustrate this dependence. The magnitude of β also modifies the radial location of the dust concentration maxima.

Fig. 2 shows the evolution of a small random Σ_d fluctuation with $\beta = 1$. The solid line denotes the final time, where we stopped the integration at the dimensionless time $t_{max} = 1$. The dotted lines are snapshots after evenly spaced periods of time. We plotted the surface density of the dust $\Sigma_d(t)$ over the dimensionless radius. These results clearly indicate the growth of the perturbed Σ_d and the formation of ringlets which are separated by gaps. The width of the rings is an increasing function of the radius because H/r increases with r . Eventually, as the amplitudes of Σ_d are strong enough, the residual disk attains an

equilibrium in which the residual dust rings become isolated.

The numerical models needed 1 dimensionless timescale to develop rings. The mean radius of the simulation was chosen to be $r = 5$ thus it took only 0.1 dimensionless orbits at the center of the dust density ring. This typical timescale can be derived from Eq. (12) and (19) to be: $\tau_0 = \left(\frac{H}{r}\right)^{-2} \frac{2\pi}{\Omega}$. If we apply parameters estimated for HR4796A (see Model A in Klahr and Lin 2001) we can estimate the time the instability needed for growth at the ring location of 70AU. The orbital period is 370 yrs. The pressure scale height is determined from the irradiation to be $H/R = 0.07$. It follows that the typical timescale is only 7.5×10^4 yrs, which means the instability developed in the model after about 10^4 yrs for the most efficient drifting particles. This model (Model A from Klahr and Lin 2003) assumes the existence of gas at an amount of $100M_{\oplus}$ in the disk around HR4796A. With such a high gas density dust grains of 600μ in size are drifting radially at the highest possible rate ($\Omega\tau_f \approx 1$ see eq. 8). The radial drift velocity decreases with the friction time and thus with gas density. In Klahr and Lin (2001) we also assumed two models (Models C and D) that contain only $10 M_{\oplus}$ respectively $1 M_{\oplus}$ in the gas. Under such conditions the instability needs 10 respectively 100 times longer. For HR4796A this means that the ring may have formed within 10^4 and 10^6 yrs depending on the amount of gas that was available. Thus, if we assume that the gas was depleted on a time scale of 10^6 yrs it is possible to generate the ring structure within this time and also to conserve or fixate the structure by removing the rest of the gas afterwards.

In Figure 3 we present the evolution of Σ_d for the $\beta = 2$ model. Maximum time was also $t_{max} = 1$. The growth of the perturbation in this case is similar to the $\beta = 1$ model though the growth rate is faster and the outward drift of the rings is more pronounced. Finally, we present in Figure 4, the evolution of Σ_d for the $\beta = -1$ model. As this process is generally slower we integrated until $t_{max} = 10$. As we have anticipated in our analytic results that an initially strong sinusoidal perturbation is damped in this case.

5. Observational Appearance

The radial dust density and temperature distribution can be translated in an intensity map via

$$I(r, \phi) \propto \Sigma_d T_d^4. \quad (21)$$

In figures 5 and 6 we show these maps for the $\beta = 1$ and $\beta = 2$ case. In the latter case the middle ring is a little wider than in the previous case. One should not expect to much difference between both cases, as β predominantly influences the timescale on which the rings form but not the structures themselves.

The resemblance to the observations of HR4796A and HD141569 is striking. Future work could focus on a possible instability of non-axisymmetric modes, which are actually already observed.

6. Conclusion

In this paper, we consider the interaction between dust, gas, and radiation in debris disks around young stellar objects. In general, the gas and the dust component do not have the same azimuthal speed. The gas attains a dynamical equilibrium in which the centrifugal force is balanced by the central stars' gravity and a negative pressure gradient in the disk. The azimuthal speed of the gas is generally sub Keplerian. In a gas-free optically-thin environment, the dust attains a dynamical equilibrium in which the centrifugal force is balanced by the central stars' gravity and a radiation pressure. In a gaseous environment, hydrodynamical drag also influences the motion of the gas and dust. In most regions of the disk where the dust concentration is relatively small, the gas causes the dust to migrate inward/outward if the azimuthal speed of the gas is smaller/larger than that of the dust.

However, in relatively massive Herbig Ae/Be stars, the UV intensity is relatively strong. Gas may be rapidly depleted through photo evaporation process (Shu, Johnstone, & Hollenbach 1993, Hollenbach *et al.* 1994). Nevertheless, a small amount of residual gas and dust may be retained around systems such as HR4796A and HD141569 for a few Myr. Regions with modest gas density and dust opacity are primarily heated by the absorption of stellar irradiation on the dust grains. The gas is indirectly heated through conduction.

We consider the evolutionary stability of a two-fluid flow under these circumstances. For simplicity, we consider the limiting case that the azimuthal speed of the gas is smaller than that of the dust initially. (Similar results can be obtained in the opposite limit). We find that in some optically thin regions of the disk, the gas temperature is an increasing function of the surface density of the dust. In this case, a slight concentration of dust leads to local pressure maxima in the gas. The positive pressure gradient interior to these maxima increases the local azimuthal velocity of the gas which remains smaller than that of the dust initially. Although the dust continues to experience a hydrodynamic drag and migrate inward, the strength of the head-wind is weaker and the inward radial velocity is smaller. Similarly, exterior to these maxima, the pressure gradient is more negative than elsewhere so that the azimuthal speed of the gas is slower than its surrounding region. This enhanced head wind causes the dust to migrate toward the maxima at a faster pace. The congestion caused by the slow down in the radial migration of the dust on the inside and the speed up on the outside of the surface density maxima in turn leads to an increase in Σ_d . This process

leads to a clumping instability.

The initial growth of the clumping instability is similar to the viscous diffusion instability in accretion disk models. But, in contrast to the viscous instability, the rings can evolve into apparently isolated entities. As the amplitude of the surface density variation increases, the modification of the local pressure distribution intensifies. Eventually, the azimuthal speed of the gas decreases below that of the dust in some region interior to the surface density maximum. The dust particles move outward as they experience a tail wind. This inflow barrier leads to the apparent isolation of the rings, while the gas distribution is merely unchanged during the entire process, but the gaseous component of the residual disk is difficult to be detected. Although this self shepherding effect diminishes with gas depletion, the diffusion of the grains due to the gas drag effect also vanishes. After the residual gas is completely evaporated, the ring structure would be preserved until particle collisions and radiation drag induces its spreading. But these processes occurs on a much longer time scale than a few Myr.

The growth rate of this clumping instability is inversely proportional to the radial wavelength of the perturbation so that it leads to the formation of concentric rings with gaps between them. The lower limit on the width of the ring is determined by the local pressure scale height. In accordance with the Rayleigh's criterion, rings with narrow widths are dynamically unstable. Although our discussion is based on the assumption that the azimuthal velocity of the gas is initially smaller than that of the dust, the same argument applies for the opposite limit. In that case it is the congestion of the dust's outward flow which causes the growth of the clumps.

Debris disks have been seen around many post T Tauri stars. Some of these systems such as β Pic have relatively smooth surface density distribution in the radial direction while those around HR4796A and HD141569 appears to have ringlet structure. While it is tempting to interpret the ringlet structure is due to the tidal interaction between the residual disk and some embedded planets, our results indicate the existence of alternative scenarios which can also account for the sharp features in the ring.

The stability condition is determined by the functional dependence of T_g on Σ_d . The instability arises when the gas temperature is an increasing function of the dust surface density. Such conditions are not satisfied in the optically thick regions of the disk or in regions where the gas molecules radiate either much more or much less efficiently than they are heated by conduction. If gas is an efficient radiator, T_g would attain the value corresponds to the ground state of the gas molecules. In the opposite limit, gas would attain the radiative equilibrium temperature of the grains. In both limits, the gas temperature becomes independent of Σ_d , $\beta = 0$, and the debris disk is stable. It is also possible that β

may attain a negative value though it seems physically unlikely. We shall examine elsewhere the functional dependence of the gas temperature on other physical parameters. This analysis will include a more realistic dust size distribution and the radiation transfer of the gas. We will also provide detailed modeling of the observations. It is entirely possible that only over some special range of disk radii that the clumping instability may arise.

We want to thank Inga Kamp for her thoroughly checking of the heating and cooling properties of optical thin disks. This work was supported by NASA TPF program under the grant NNG04G191G. Work supported in part by the European Community's Human Potential Programme under contract HPRN-CT-2002-00308, PLANETS.

A. Gas Temperature Estimate

For this work we assumed a temperature versus dust density relation with a positive slope, without further discussing the exact shape of this relation. A detailed exact derivation would need the use and modification of a radiation transfer code (see Kamp & van Zadelhoff 2001; Ferland, Korista, Verner, Ferguson, Kingdon & Verner 1998; Woitke, Krüger & Sedelmayr 1996). This shall not be done here.

But we can derive some general expressions for the gas temperature (T) as it depends on the surface area that is provided by the dust grains. The strongest heating Q^+ provided to the Hydrogen molecules probably occurs by photoelectric heating via the silicate grains (Kamp & van Zadelhoff 2001):

$$\Gamma_{pe} = 2.5 \times 10^{-4} \sigma \epsilon \chi n_{\text{H}}. \quad (\text{A1})$$

Here $\sigma = \frac{n}{n_{\text{H}}} \sigma_d$ is the total grain cross section per H nucleus, ϵ is the photoelectric efficiency, and χ is the intensity of the UV field from the central object (σ_d is the cross section and n the number of dust grains).

Actually ϵ also depends on the gas temperature, but for the expected low temperatures $T_g \ll 10^4 \text{K}$ this dependence is negligible for our purpose. ϵ depends on n_e and χ and hence using reasonable values of those two, e.g. $n_e = 1 \text{cm}^{-3}$, $\chi = 300$ at 70 AU, ϵ can only vary as much as by a factor 2 between 10 and 100 K.

Thus it follows, that the heating is in first order linear increasing with the number of the dust grains:

$$\Gamma_{pe} \propto n. \quad (\text{A2})$$

The Hydrogen being at its ground state can not cool via radiation but only via collisions with other atoms or molecules. These collision partners themselves will cool via rotational or fine structure transitions (Woitke et al. 1996). Given the strong UV radiation field of a young A0 V star, the dominant cooling agent is probably ionized carbon CII (Kamp *et al.* 2003). One can expect that C is totally ionized and $n_{C+} \propto 10^{-4}n_{\text{H}}$. We use the two level approximation of Hollenbach & McKee (1989) for the ground state of the ionized carbon: It is the 157.5μ line that has a cooling rate of:

$$\Lambda_2 = f_1 n(\text{CII}) A_{10} h \nu_{10}. \quad (\text{A3})$$

The fraction of CII in the upper level can be calculated via

$$f_1 = \frac{g_1 e^{-E_1/kT}}{g_0 + g_1 e^{-E_1/kT}}, \quad (\text{A4})$$

with the statistical weights $E_0 = 0.0$ and $E_1 = 1.27 \times 10^{-14}$ and $g_0 = 2, g_1 = 4$ respectively. A_{10} is the Einstein probability for spontaneous emission. When the heating is balanced by cooling, we can calculate the dependence of equilibrium temperature on the number of dust grains:

$$\frac{g_1 e^{-E_1/kT}}{g_0 + g_1 e^{-E_1/kT}} \propto \frac{n}{n_{\text{H}}} \quad (\text{A5})$$

which can be easily solved for T . In Fig. 2 we plot the dependence of T/T_0 on n/n_0 . The exact values for T_0 and n_0 have to be calculated model dependent, but we already see that β in this plot is roughly 1.0 (which is independent on the explicit model) and we conclude that the instability can occur on reasonable timescales.

REFERENCES

Agnor, C. B. & Ward, W. R. 2002, ApJ, 567, 579

Armitage, P.J., Livio, M., Lubow, S.H., & Pringle, J.E. 2002, MNRAS, 334, 248

Artymowicz, P., & Lubow, S.H. 1994, ApJ, 421, 651

Artymowicz, P. & Lubow, S. H. 1996, ApJ, 467, L77

Borderies, N., Goldreich, P., & Tremaine, S. 1989, Icarus, 80, 344

Boss, A. 1998, ApJ, 503, 923

Bryden, G., Ro'zyczka, M., Lin, D.N.C., & Bodenheimer, P. 2000, ApJ, 540, 1091

Bryden, G., Chen, X., Lin, D.N.C., Nelson, R.P., Papaloizou, J.C.B. 1999, *ApJ*, 514, 344

Chiang, E.I., & Goldreich, P. 1997, *ApJ*, 460, 368

Ferland, G. J., Korista, K. T., Verner, D. A., Ferguson, J. W., Kingdon, J. B., & Verner, E. M. 1998, *PASP*, 110, 761

Goldreich, P., & Tremaine, S. 1982, *ARA&A*, 20, 249

Goldreich, P., & Tremaine, S. 1980, *ApJ*, 241, 425

Haisch, K.E., Jr., Lada, E.A., & Lada, C.J. 2001, *ApJ*, 553, L153

Hollenbach, D. & McKee, C. F. 1989, *ApJ*, 342, 306

Hollenbach, D., Johnstone, D., Lizano, S., & Shu, F. 1994, *ApJ*, 428, 654

Ida, S., Bryden, G., Lin, D.N.C., & Tanaka, H. 2000, *ApJ*, 534, 428

Ida, S., & Lin, D.N.C. 2003, *ApJ*, in press

Johnson, B. M. & Gammie, C. F. 2003, *ApJ*, 597, 131

Kamp, I. & van Zadelhoff, G.-J. 2001, *A&A*, 373, 641

Kamp, I., van Zadelhoff, G.-J., van Dishoeck, E. F., & Stark, R. 2003, *A&A*, 397, 1129

Klahr, H., & Lin, D.N.C. 2001, *ApJ*, 554, 1095

Larwood, J.D. & Papaloizou, J.C.B. 1997, *MNRAS*, 285, 288

Lin, D.N.C., & Papaloizou, J. 1986, *ApJ*, 307, 395L

Lin, D.N.C., & Papaloizou, J. 1986, *ApJ*, 309, 846

Lin, D.N.C., Bodenheimer, P., & Richardson, D.C. 1996, *Nature*, 380, 606

Lin, D. N. C. & Ida, S. 1997, *ApJ*, 477, 781

Marcy, G.W., Butler, R.P., & Vogt, S.S. 2000, *ApJ*, 536, L43

Masset, F.S., & Papaloizou, J. 2003, 588, 494

Mayor, M., & Queloz, D. 1995, *Nature*, 378, 355

McCabe C., Duchene G., & Ghez A.M., 2003, *ApJ*, 588, 113

Nelson, A.F., Benz, W., Adams, F.C., & Arnett, D. 1998, *ApJ*, 502, 342

Pollack, J.B., Hubickyj, O., Bodenheimer, P., Lissauer, J.J., Podolak, M., & Greenzweig, Y. 1996, *Icarus*, 124, 62

Papaloizou, J., & Lin, D.N.C. 1984, *ApJ*, 285, 818

Pickett, B.K., Mejia, A.C., Durisen, R.H., Cassen, P., Berry, D.K., & Link, R.P. 2003 *ApJ*, in press

Pickett, B.K., Durisen, R.H., Cassen, P., & Mejia, A.C. 2000 *ApJ* 540, L95

Pringle, J. E. 1981, *ARA&A*, 19, 137

Schneider, G., Smith, A.S., Becklin, E.E., Koerner, D.W., Meier, R., Hines, D.C., Lowrance, P.J., Terrile, R.J., Thompson, R.I., & Rieke, M. 1999, *ApJ*, 513, 127

Sheret, I., Ramsay Howat, S. K., & Dent, W. R. F. 2003, *MNRAS*, 343, L65

Shu, F. H., Johnstone, D., & Hollenbach, D. 1993, *Icarus*, 106, 92

Stauffer, J.R., Prosser, C.F., Hartmann, L. & McCaughrean, M.J. 1994, *AJ*, 108, 1375

Takeuchi, T., & Artymowicz, P. 2001, *ApJ*, 557, 990

Thi, W. F. et al. 2001, *ApJ*, 561, 1074

Thi, W. F., Pontoppidan, K. M., van Dishoeck, E. F., Dartois, E., & d'Hendecourt, L. 2002, *A&A*, 394, L27

Thommes, E. W., Duncan, M. J., & Levison, H. F. 2002, *AJ*, 123, 2862

Trilling, D.E., Lunine, J.I., & Benz, W. 2002, 394, 241

Ward, W.R. 1986, *Icarus*, 67, 164

Weidenschilling, S.J. 1977, *MNRAS*, 180, 57

Weinberger, A.J., Becklin, E.E., Schneider, G., Smith, B.A., Lowrance, P.J., Silverstone, M.D., Zuckerman, B., & Terrile, R.J. 1999, *ApJ*, 525, 53

Woitke, P., Krueger, D., & Sedlmayr, E. 1996, *A&A*, 311, 927

Yorke, H. W. & Sonnhalter, C. 2002, *ApJ*, 569, 846

Zuckerman, B., Kim, S.S., & Liu, T. 1995, *ApJ*, 446, L79

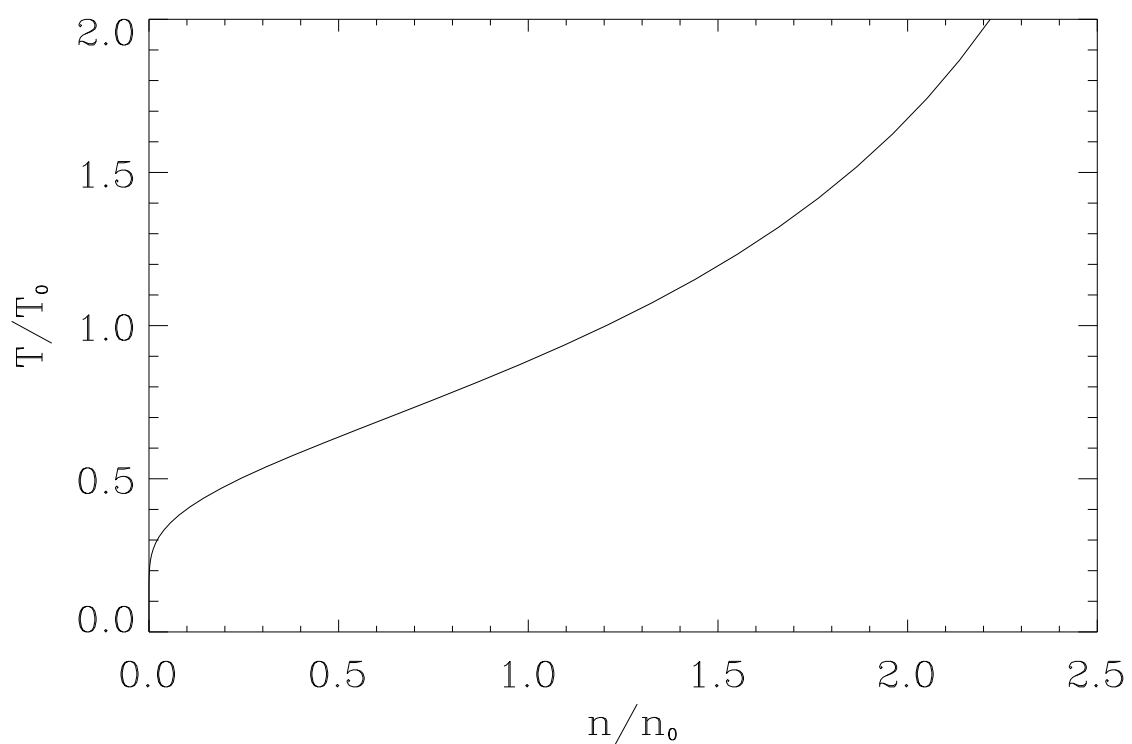


Fig. 1.— Exemplary temperature dependence of the gas on the number of dust grains. See text for details.

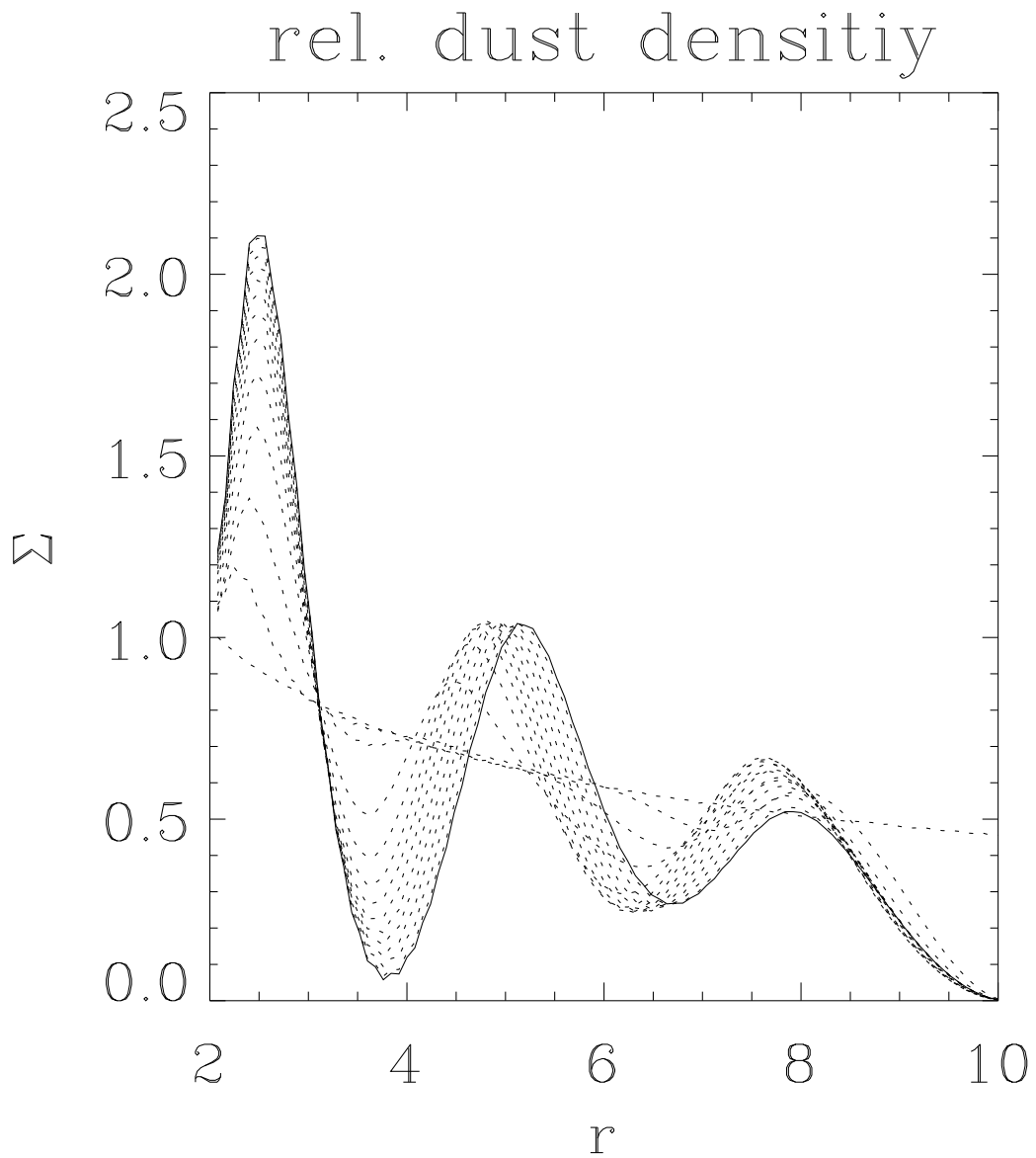


Fig. 2.— Evolution of an initially homogeneous dust distribution over dimensionless time $t = 1$ in units of the initial value over the dimensionless radius. $\beta = 1$.

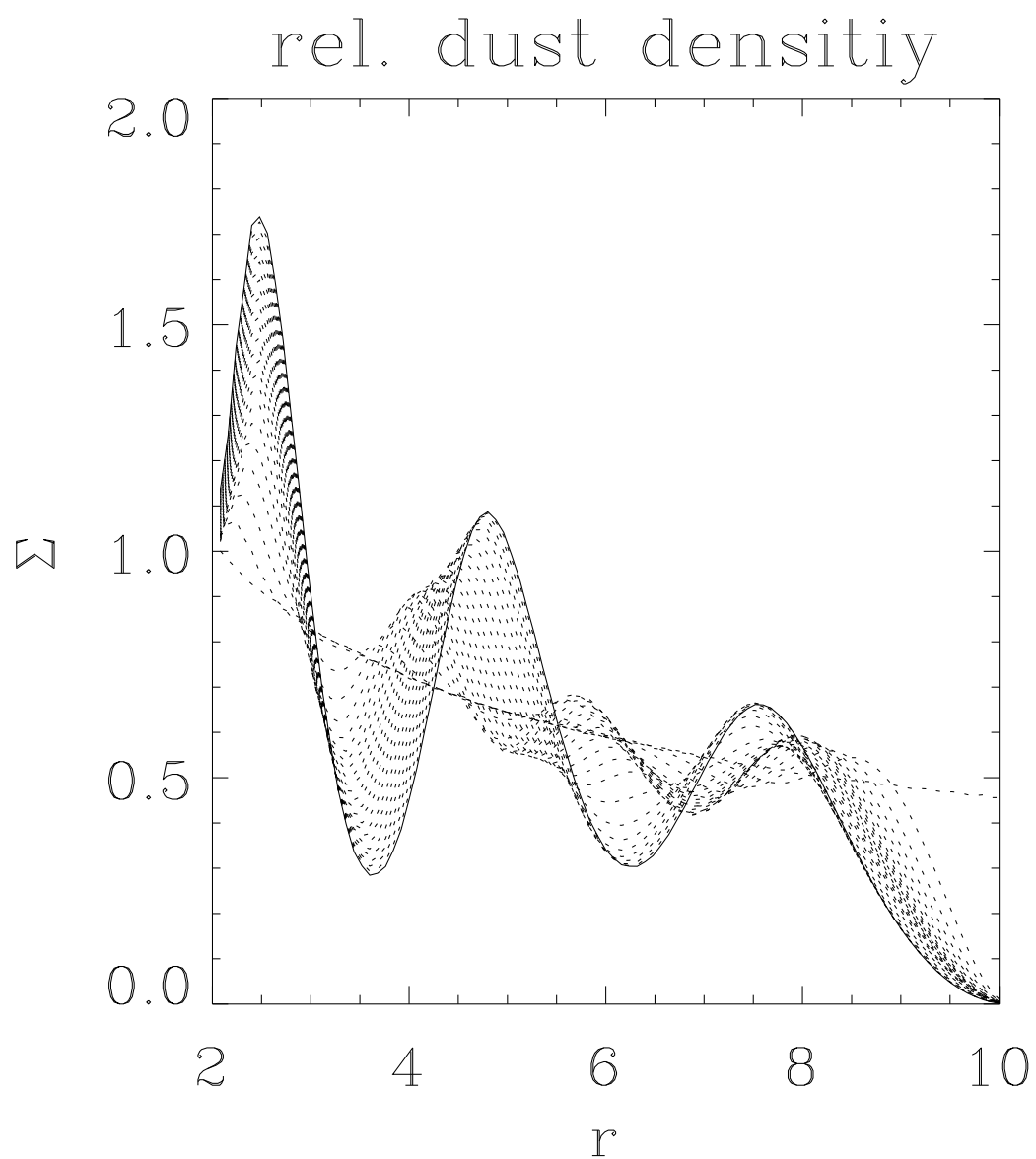


Fig. 3.— Evolution of an initially homogeneous dust distribution over dimensionless time $t = 1$ in units of the initial value over the dimensionless radius. $\beta = 2$.

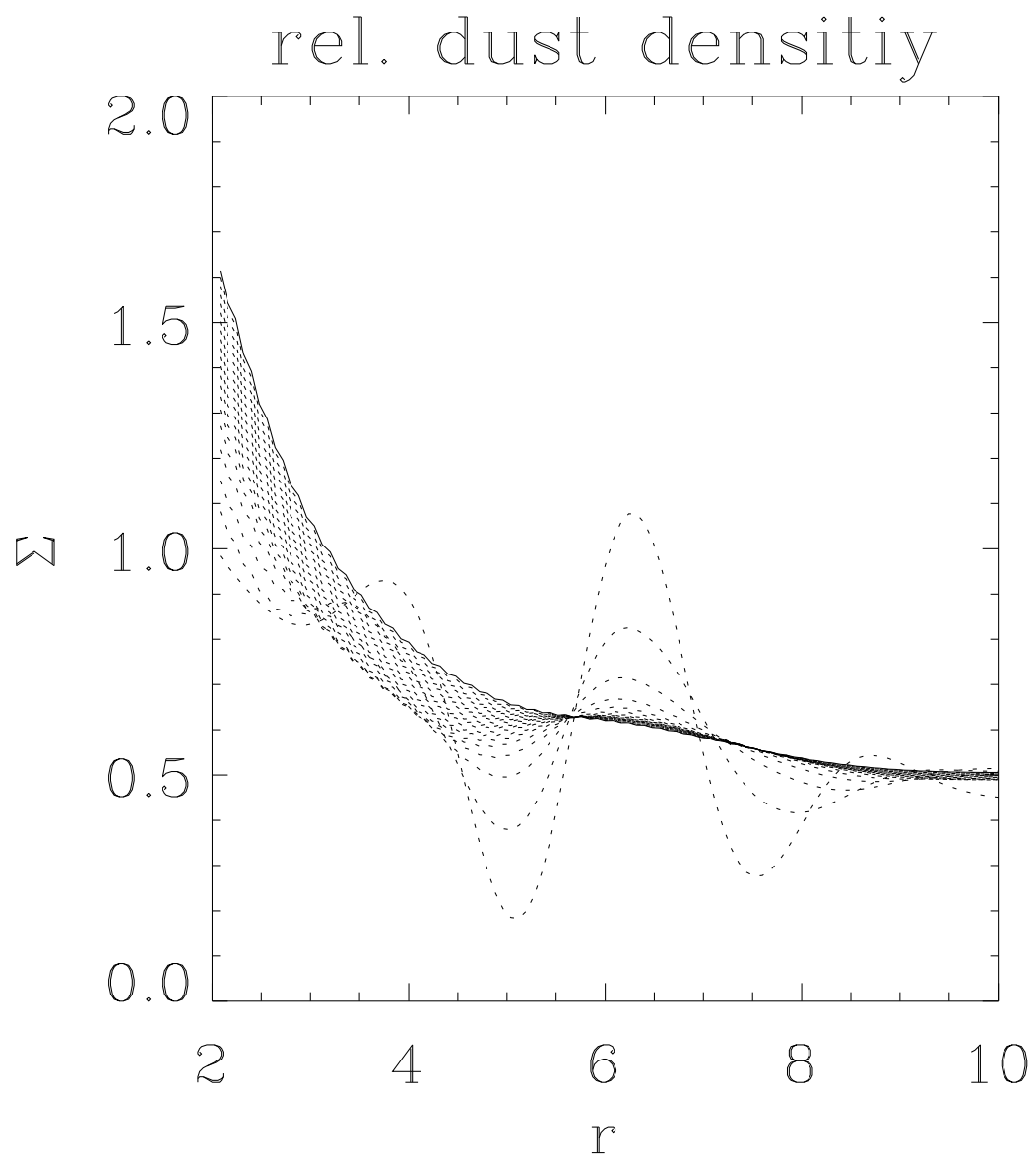


Fig. 4.— Evolution of an initially sinusoidal dust distribution over dimensionless time $t = 10$ in units of the initial value over the dimensionless radius. $\beta = -1$.

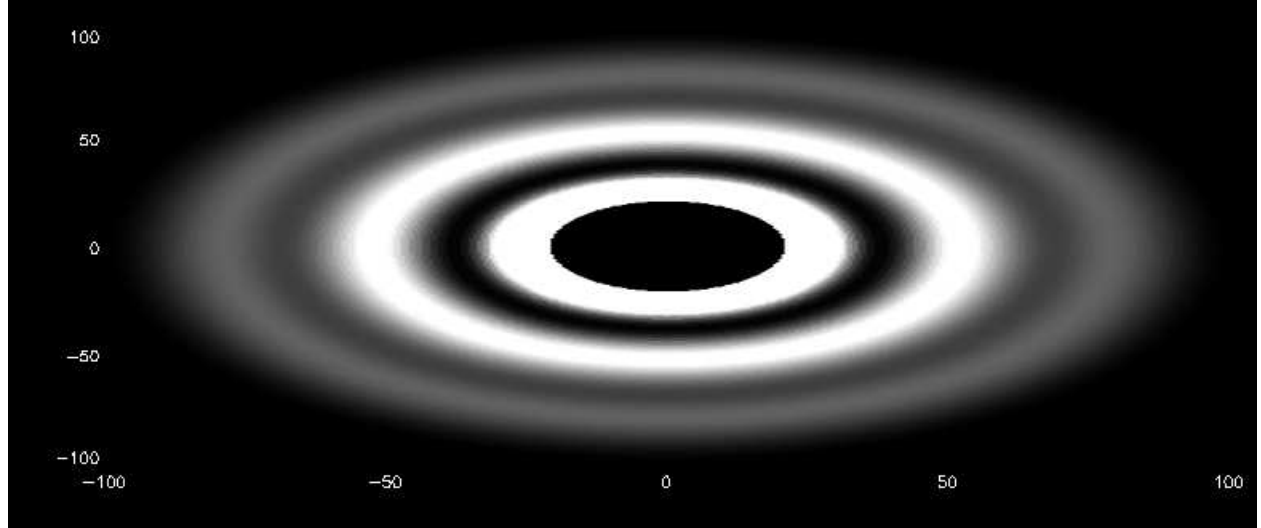


Fig. 5.— Simulated intensity map for an optical thin debris disk. $\beta = 1$.

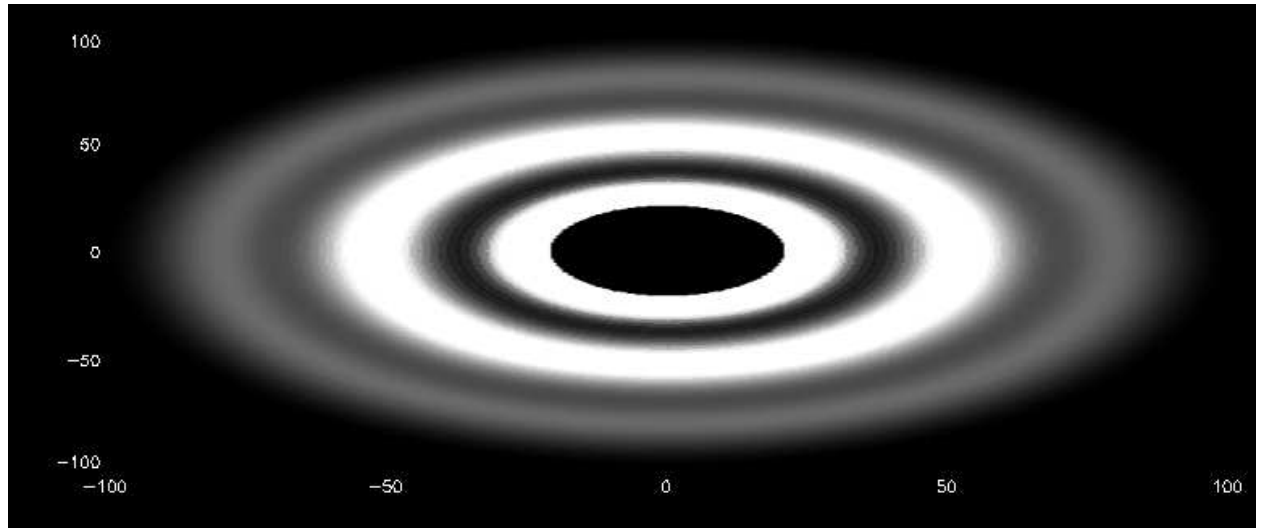


Fig. 6.— Simulated intensity map for an optical thin debris disk. $\beta = 2$. Now the middle ring is wider than in the previous case.